

The Possible Ameliorating Effect of Allicin (Oral\Inhalation) on Cadmium Induced Acute Lung Injury in Adult Male Albino Rats: Histological and Immunohistochemical Study

Original
Article

Amira Fathy Ahmed, Reham Mohamed Abo Eliel, Sahar Ahmed Mokhmer and Soha Abdel- kawy Abdel- Wahab

Department of Histology and Cell Biology, Faculty of Medicine, Minia University, Egypt

ABSTRACT

Introduction: Proper therapy of acute lung injury (ALI) is a major health challenge nowadays; it represents the most serious complication of COVID19 and the main cause of death. There are accumulating studies about the possible therapeutic effects of Allicin, the active ingredient of garlic, in many cases of respiratory diseases.

Aim of the Work: In the current study, we showed for the first time a novel route of administration of Allicin which markedly improves its therapeutic effects in induced animal model of ALI.

Material and Methods: Forty adult male albino rats were divided equally into control group, animal model group with cadmium inhalation for induction of ALI, recovery group left without treatment, and two treated group. Allicin was given as a treatment by two different routes, orally and through nebulizer inhalation in a dose of 200 mg/kg.

Results: Cadmium chloride (CdCl_2) inhalation induced nearly the same histopathological changes in the animal lung tissue in the form of inflammation, congestion and vasculitis as that reported in covid-19 autopathic biopsy. Allicin markedly improved these deleterious effects through nebulizer inhalation; it induced significant lowering in IL-6, iNOS and malonaldehyde with significant increase in the number CD163 positive anti-inflammatory macrophage. Moreover, it stimulated type II pneumocyte regeneration and this detected by TrkB proliferation marker. The level of antioxidant reduced glutathione showed significant increase with allicin inhalation. Lung histological architecture markedly improved and nearly back to normal after allicin inhalation.

Conclusion: We concluded that allicin through nebulizer inhalation may be of great help in the management of critical cases with acute lung injury.

Received: 27 October 2022, **Accepted:** 28 November 2022

Key Words: Acute lung injury, allicin, inhalation, oral.

Corresponding Author: Amira Fathy Ahmed, MD, Department of Histology and Cell Biology, Faculty of Medicine, Minia University, Egypt, **Tel.:** +20 11 2276 0040, **E-mail:** amirafathy332@gmail.com

ISSN: 1110-0559, Vol. 47, No. 1

INTRODUCTION

Acute lung injury (ALI) is a serious lung disease with high rate of morbidity and mortality^[1]. In cases of viral infection, as in coronavirus (CoV), cytomegalovirus (CMV), adenovirus, influenza virus, and respiratory syncytial virus (RSV), gas-exchange function of the lung alveoli is seriously affected^[2,3]. Cadmium chloride (CdCl_2) is a pollutant affecting the human health^[4] because of its bio-accumulative nature^[5].

Histopathological changes induced CdCl_2 inhalation including acute pulmonary damage, pneumonitis, pulmonary emphysema, surfactant synthesis affection, interstitial lung diseases^[6] mimic the pulmonary changes of acute viral infection^[7]. These detritus effects of CdCl_2 inhalation are most properly caused by lung tissue inflammation and pneumocyte type II injury^[8].

Allicin (diallylthiosulfinate) is the principal active component in garlic and acts as a natural defense substance^[9]. Allicin has a bactericidal effect, antifungal, anti-inflammatory and hypolipidemic activities^[10].

In vitro study done by^[11] reported that allicin can inhibit SARS- COV-2 replication and enhances the antiviral host responses in the Calu-3 pulmonary cells line. Furthermore accumulated data from previous studies, showed that it possesses antiviral activity against many viruses including Coronavirus (CoV)^[12].

Inhalation of allicin vapors or aerosols potentially offers a direct route for ameliorating lung inflammation caused by various types of lung pathogens^[13].

In this study we hypothesized that allicin inhalation may be of curative effect in cases of corona virus (cov-2) ALI and we compared the potency of these effects via two different routes of administration orally and by inhalation.

MATERIALS AND METHODS

Animals

In the current study, forty adult male albino rats were used, their weights were ranging between 150-180gm. This study was performed in accordance to the guidelines approved by the EL-Minia University institutional Ethical Committee for laboratory animals.

Reagents

1. Cadmium chloride (CdCl₂) Monohydrate 98% pure powder (catalog no. 02416000100) purchased from Sigma Company, Egypt.
2. Allicin (Allimax capsule) 180 mg was purchased from Amazon application, USA.
3. Anti-inducible Nitric oxide synthase (iNOS) anti-body monoclonal mouse antibody, (catalog no. PA1-036 1:20) obtained from Thermo Fisher Company, USA.
4. CD163 monoclonal mouse antibody, (catalog no. GTX35247 1:100) obtained from Gene Tex Company, USA.

Experimental design

In this study, 4 animals were housed a separate cage, with free access for water and chew, in air-conditioned room^[14]. The cadmium chloride and allicin aerosol were propelled by the nebulizer into a glass chamber, with 60 cm × 40 cm × 40 cm dimensions each 4 rats were allowed to move freely during the exposure. Two small side wall openings (diameter of 1 cm) in the chamber were required for a regular distribution of the aerosol^[15].

The experimental animals were randomly divided into five groups each group with 8 rats as the following:

Group I (Control group): This group was formed of 8 rats were divided equally in to 2 subgroups: A) subgroup A: each one received 1ml of 0.9 NaCl saline orally once daily for 10 days. B) subgroup B: each one received nebulized 1ml of 0.9 NaCl saline for 1h once daily^[16]

Group II (Cadmium chloride (CdCl₂), acute lung injury group): This group received 0.1 mg / kg of CdCl₂ dissolved in 4ml 0.9 % NaCl saline via nebulizer^[15]. for 2h per day for 3 days^[17]. Each session of CdCl₂ inhalation was divided into 4 sub-sessions, each was about half an hour to decrease the mortality rate.

Group III (Recovery group): This group received CdCl₂ as in group II then left without treatment for 7 days.

Group IV (Allicin oral group): This group received CdCl₂ as in group II then each rat received allicin 200 mg/kg orally dissolved in 1 ml 0.9 % NaCl saline once daily^[18] for 7 days^[19].

Group V (Allicin inhalation group): This group received CdCl₂ as in group II then received 200 mg/kg of allicin dissolved in 4 ml 0.9 % NaCl saline via nebulization for 1h once daily for 7 days.

After 3 days for the CdCl₂ group and after 10 days for the other groups, rats were anaesthetized by light halothane and scarified by decapitation. Lung Specimens were carefully dissected for tissue preparation. After rinsing in normal saline, pieces of lung tissues were put in cassettes to avoid lung floating then rapidly fixed in 10% formaldehyde saline for 48 hours, then washed by water and

proceeded to prepare paraffin sections 5 μm thickness for the histological, immunohistochemical and morphometric studies. Other lung specimens were either used for tissue homogenates preparation for the biochemical study or immediately fixed in 2.5% glutaraldehyde for electron microscopic study.

Biochemical study

Biochemical analysis was done at the Pharmacology Department, Faculty of Medicine, EL-Minia University.

Measurement of tissue malondahyde (MDA) and reduced glutathione (GSH)

Lung specimens were weighed, homogenized in ice cold PBS (pH 7.4) and centrifuged. The resulting supernatant was collected to assess lung MDA (marker for lipid peroxidation) and GSH (antioxidant marker) using commercially available kits (Bio diagnostic, Egypt) according to manufacturer's instructions

Measurement of tissue Tropomyosin Receptor Kinase B (TrkB) and interleukin 6 (IL6)

Tissue specimens were weighed and then homogenized in PBS on ice. Levels of TrkB (proliferation marker)^[20] (Catalogue number NBP2-76777, NOVUS, USA) and Interleukin 6 (proinflammatory cytokine)^[21] (Catalogue number E-EL-R0015 96T, Elabscience, USA) were measured by a quantitative enzyme-linked immunosorbent assay (ELISA) kits according to the manufacturer's instructions.

Histological studies

Hematoxylin and Eosin (H&E) stains^[22] and Masson's trichrome staining^[23]

Lung tissue specimens were processed to prepare paraffin sections 5μm thickness and ordinary histological staining (H & E and Masson trichrome staining). In brief, samples were fixed in 10% formalin, embedded in paraffin and dehydrated in ascending concentrations of ethyl alcohol (70%-100%).

Immunohistochemical study^[22]

Immunocytochemical staining was performed according the manufacture protocol using anti iNOS anti-body as a marker for cell inflammation and anti-CD 163 anti-body as a marker for anti-inflammatory (M2) macrophages.

4-5μm paraffin sections were deparafinized by xylene and tissue rehydrated by descending grades of alcohol were done. Antigen retrieval was done by boiling in 10mm citrate buffer solution (PH 6) for 20 min. For blocking of endogenous peroxidase enzyme, sections were kept in 0.1% H₂O₂ for 15 minutes. Sections were rinsed by phosphate buffer solution and incubated in antiserum at room temperature for 5 minutes to avoid high background. Incubation with the diluted primary antibodies for anti-iNOS antibody 1:20 and anti-CD 163 antibody 1:100 was done. Sections then were washed and incubated for

30 minutes with biotinylated goat anti-rabbit secondary antibodies diluted 1:1000. The reaction was developed with detection System (ultra-vision one), HRP Polymer & DAB Chromogen (Thermo Fisher Company, USA). After fulfillment of the reaction, counterstaining was performed with the usage of Meyer's hematoxylin. Finally, the slides were covered by Coverslip. In negative control specimens, previous steps were performed except the primary antibodies were not added.

Transmission electron microscopic study

Lung specimens were immersed in 2.5% glutaraldehyde for fixation in 0.1 ml cacodylate buffer at pH 7.4 for 24h at 4 °C, then washed with in 1% osmium tetroxide in distilled water at 4°C. Dehydration was done then the sections were embedded in epoxy resin. Semithin sections of 1 µm were prepared and stained with toluidine blue. Ultrathin sections (80 nm) were placed on grids and stained for examination. Previous procedures (preparations of semithin and ultrathin sections and examination of the stained sections) were done in EL-Minia University Central Laboratory for Nanotechnology and Microanalysis.

Photography

Examining and capturing images were done by light microscopy B X 51 (Olympus, Japan) connected to LC micro application software program, at Faculty of Medicine – EL-Minia University at Histology and Cell Biology Department.

Ultra-structural images were photographed using transmission electron microscopy (JEM-100CX II, Japan).

Morphometric study

- The mean surface area fractions of collagen fibers and iNOS immune reactivity were assessed.
- The mean numbers of CD163 positive anti-inflammatory macrophages were assessed.

All previously mentioned morphological parameters were assessed in 8 adjacent nonoverlapping fields from each rat of the different groups (n=8). Collagen area fractions were measured at 100 magnifications, while other parameters were assessed at 400 magnifications. Examination of different experimental groups was done by blind eye histologist.

For image analysis, Image J software (<http://rsbweb.nih.gov/ij/>; NIH, Bethesda) was used.

Data handling and statistical analysis

SPSS (IBM Corp. Released 2010. Windows, Version 19.0) was used for quantitative data analysis. The mean and standard deviation (SD) was calculated for the parameters of each group. Values were expressed as means ± SD. One-way analysis of variance (ANOVA) test was used for the detection of significant differences between groups, followed by the use of LSD as a post hoc test. The statistically significant results assessed when the *p*-values were <0.05.

RESULTS

Biochemical results

Effect of allicin on MDA and IL-6 levels in the lung tissue of CdCl₂ induced acute lung injury rats

The levels of MDA (Figure 1A) and IL-6 (Figure 1C) were significantly increased in CdCl₂ group compared to the control group. However, allicin administration as oral or inhalation caused significant decrease in their levels in comparison to the CdCl₂ group. Interestingly, allicin inhalation reversed the effects of CdCl₂ on MDA levels which showed insignificant difference compared to the control group, on the other hand IL-6 levels still significantly higher than control.

Effect of allicin on the GSH and TrkB levels in the lung tissue of CdCl₂ induced acute lung injury rats

The level of GSH (Figure 1B) and TrkB (Figure 1D) significantly decreased in CdCl₂ group compared to the control group. Allicin administration as oral or inhalation significantly increased GSH and TrkB levels when compared to the CdCl₂ group. Allicin inhalation had more obvious effect in increasing GSH and TrkB levels compared to allicin oral group with insignificant difference with control group.

The histological results

Hematoxylin and eosin results

The control group showed normal histological appearance of the lung tissue, with patent alveoli and alveolar sacs lined with flat numerous cells (pneumocytes type I) and less numerous rounded cells protruded into the alveolar lumen (pneumocyte type II). Delicate interalveolar septa with blood capillaries and macrophages was observed (Figures 2 A,B). Normal bronchiolar epithelium, simple columnar ciliated epithelium, with the surrounding circularly arranged smooth muscle cells were observed (Figure 2 C).

In CdCl₂ group, the lung showed distorted alveoli with abnormal lining. Thickened interalveolar septa showed congestion and infiltration with inflammatory cells (neutrophils, macrophages, and lymphocytes) and areas of hemorrhages. Numerous fibroblasts were noticed in the interstitial tissue and around the bronchioles (Figures 3 A,B,C). Bronchiolar epithelium revealed stratification with discontinuous and separated epithelium from its basement membrane with presence of apoptotic cells in its lumen. Interrupted musculosa was observed (Figure 3 D).

As regard the recovery group, distortion of normal lung architecture was evident. Some alveoli began to form acidophilic homogenous material in their lumina. PII were frequently observed. Numerous multinucleated giant cells and hemosiderin laden macrophages were obvious (Figures 4 A,B). Bronchiole showed desquamated epithelium with residual cells on denuded basement

membrane. Marked inflammatory cells infiltration was still obvious in the interstitium (Figure 4 C).

After 7 days of oral administration of allicin, there was partial restoration of normal lung architecture. Compartmentalization of the Alveolar sacs by low ridges were observed. Cellular proliferation of alveolar epithelium was recognized in some alveoli. Mild vascular congestion and inflammatory cellular infiltration in the interstitium except around bronchioles were noticed (Figures 5 A,B). Partially restored bronchiolar epithelium with presence of flat cells among the epithelial cells were observed. Few desquamated epithelial cells and macrophages were observed in the bronchiolar lumen (Figure 5 C).

While 7 days after allicin inhalation, the lung architecture appeared regenerated and restored. Alveolar epithelium appeared restored with minimal inflammatory cellular infiltrations, vascular congestion or dilatation (Figures 5 D,E). Apparently normal bronchiolar epithelium with restored mucosal folding was noticed with continuous circularly arranged smooth muscle layer (Figure 5 F).

Masson trichrome stain

Masson trichrome stained lung sections which detect collagen deposition (blue color) showed significant increase in area fraction of collagen deposition especially around bronchioles and blood vessels in CdCl₂ and recovery groups. However, oral and inhalation allicin groups showed significantly lower collagen deposition compared to CdCl₂ group but still significantly higher than control group (Figures 6 A-F).

Immunohistochemical study

Immunostaining of the lung tissue of different groups with an antibody specific for iNOS showed a significant increase in the mean area fraction of iNOS immunopositive cells in CdCl₂ and recovery groups compared with all other groups. In addition, there was a significant decrease in the mean area fraction of iNOS expression in allicin inhalation group in comparison to allicin oral group (Figures 7 A-F).

As regard CD163, an antibody specific for M2

macrophages, there was a significant increase in the mean number of CD163 positive cells in CdCl₂, recovery, allicin oral and inhalation groups compared to control group. While in allicin oral and inhalation groups, there was a significant increase CD163 immunopositive cells compared to CdCl₂ and recovery groups. Moreover, there was a significant increase CD163 positive cells in allicin inhalation group compared to allicin oral group (Figure 8 A-F).

Ultrastructural study using transmission electron microscopy

A. Type II pneumocyte

The control group showed numerous rounded to oval surfactant lamellar bodies with euchromatic nucleus. CdCl₂ group showed empty lamellar bodies and heterochromatic nucleus with wide perinuclear space. The recovery group showed many irregular lamellar bodies with indistinct lamellation and shrunken heterochromatic nucleus with disrupted nuclear membrane. The allicin oral and inhalation groups showed some lamellar bodies filled with surfactant while the others appeared with indistinct lamellation (Figures 9A,9B,9C,9D,9E).

B. Blood air barrier

Control group revealed intact capillary endothelium, type-I pneumocyte with thin attenuated cytoplasm and fused basement membrane of the endothelial cell and type-I pneumocyte. CdCl₂ group showed discontinuous capillary endothelium with vacuolated cytoplasm and swollen mitochondria with degenerated cristae and degenerated type I pneumocyte. The recovery group showed out sprout of the endothelial cell membrane and degeneration of type I pneumocyte. Allicin oral group showed small cytoplasmic vacuoles in the endothelial cell however, fused basement membrane between endothelial cell and type-I pneumocyte was evident. Allicin inhalation group revealed apparently normal endothelium and type I pneumocyte with thin attenuated cytoplasm. Fused basement membrane between endothelial cell and type-I pneumocyte was noticed (figures 9F,9G,9H,9I,9J).

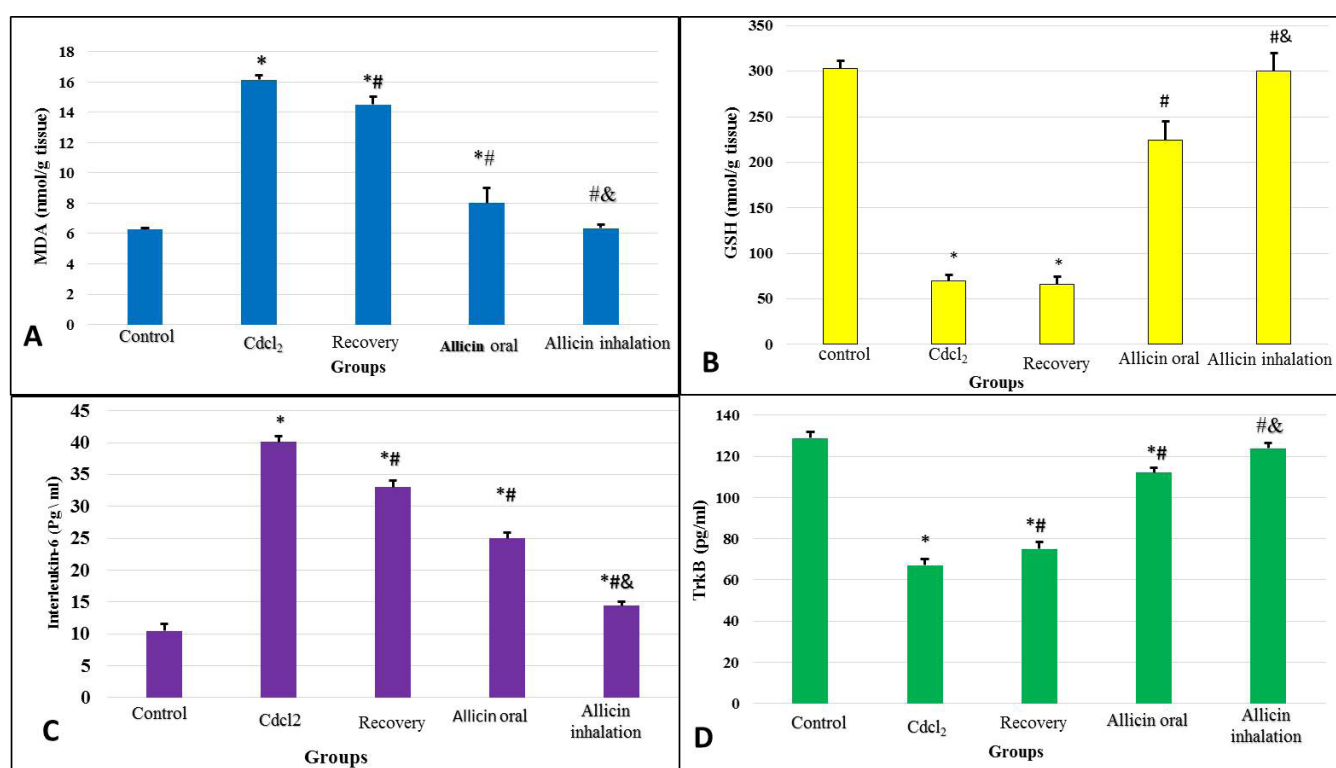


Fig. 1: Effect of allicin on the mean levels of A) Malonaldehyde (MDA), B) reduced glutathione (GSH), C) interleukin-6 (IL-6) and D) tropomyosin receptor kinase B (TrkB) in lung tissues in the studied groups (n = 8). * Significant vs: Control group, # Significant vs: Cdcl₂ group, & Significant vs: allicin oral group; significant at $p \leq 0.05$.

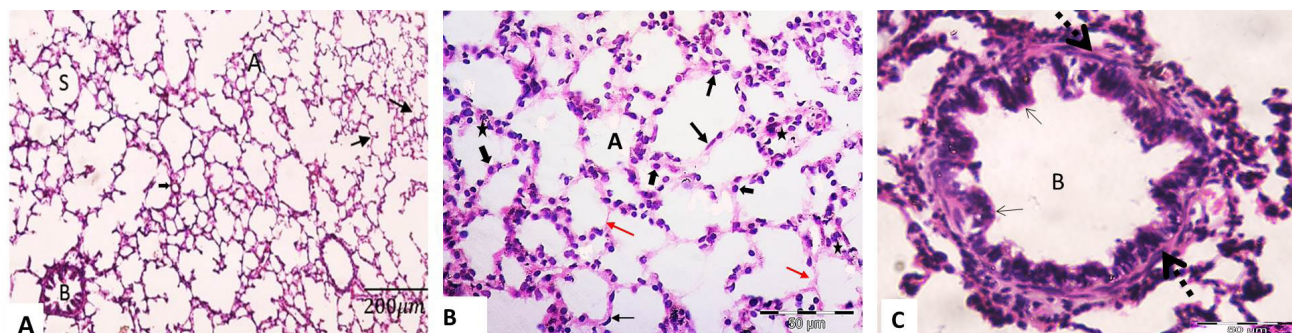


Fig. 2: Representative photomicrographs of adult male albino rat lung tissue of the control group showing A) Alveoli (A) with thin inter-alveolar septa (black arrows), alveolar sacs (S), bronchiole (B) and blood capillaries (thick arrow). B) The alveoli (A) appear as several connected pouches, pneumocyte type I (black arrows), type II (thick arrows) and alveolar macrophages (black star) in the thin interalveolar septum (red arrows). C) Bronchiole (B) with normal folded simple columnar ciliated epithelium (black arrows) with normal circular muscle layer (dotted arrows). H&E: A X100; B, C X400

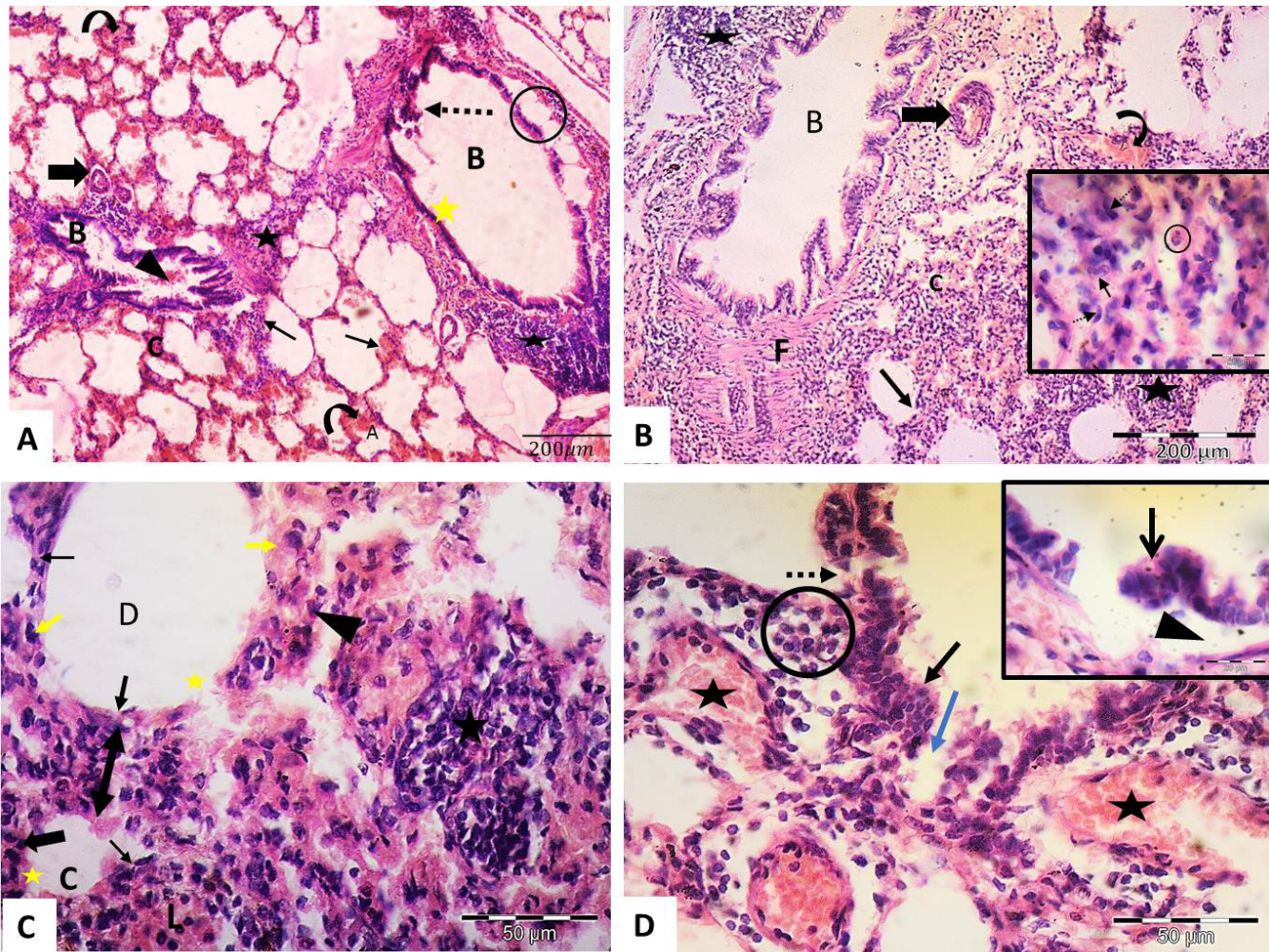


Fig. 3: Representative photomicrographs of adult male albino rat lung tissue of CdCl₂ group showing: A, B) Areas of hemorrhage (curved arrows), collapsed alveoli filled with extravasated RBCs (C) with thick inter-alveolar septa studded with extravasated RBCs and inflammatory cells (thin arrows). Notice dilated bronchiole (B) with detached (black circle) and sloughed epithelial lining (dotted arrow). Congested blood vessels (thick arrows) with marked inflammatory cellular infiltration (black stars). Notice inset showing neutrophils (circle), macrophages (arrow) and fibroblast (dotted arrows). C) Some alveoli are collapsed (C) while the others are dilated (D). Notice loss of continuity of the alveolar epithelium (yellow stars), pneumocyte type I (thin black arrows), type II (thick arrows) with pyknotic nuclei and numerous alveolar (yellow arrows) and interstitial macrophages (arrowhead). D) Bronchiole with stratification of its epithelium (black arrow and inset), discontinuous epithelium (blue arrow), epithelial separation from its basement membrane (arrowhead in inset) and interrupted muscosa (dotted arrow). H&E: A, B X100; C, D X400; inset X1000

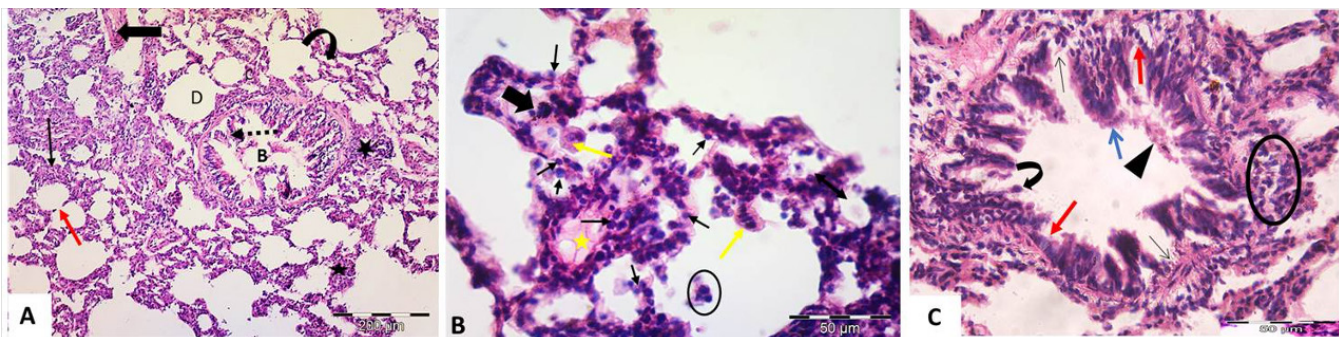


Fig. 4: Representative photomicrographs of adult male albino rat lung tissue of the recovery group showing: A) collapsed (curved arrow) and dilated (D) alveoli with thick inter-alveolar septa studded mononuclear inflammatory cells (thin black arrow) in some areas and discontinuous interalveolar septum in other areas (red arrow). Notice the lumen of the bronchiole (B) containing exfoliated epithelial cells (dotted arrow) and congested blood vessels (thick arrows) with inflammatory cellular infiltration (black stars). B) Some alveoli containing acidophilic homogenous material (yellow star) and others contain inflammatory cells (black circle). Numerous multinucleated giant cells (yellow arrows) and hemosiderin laden macrophages (thick arrow) are observed. Notice pneumocyte type II (thin black arrows) are frequently observed. C) Bronchiole with desquamated (blue arrow) epithelium with residual cells (red arrows) on denuded basement membrane (thin black arrows). Macrophage (curved arrow) and cellular debris (arrowhead) in the bronchiolar lumen. Inflammatory cells infiltration (black circle). H&E: A X100; B, C X400

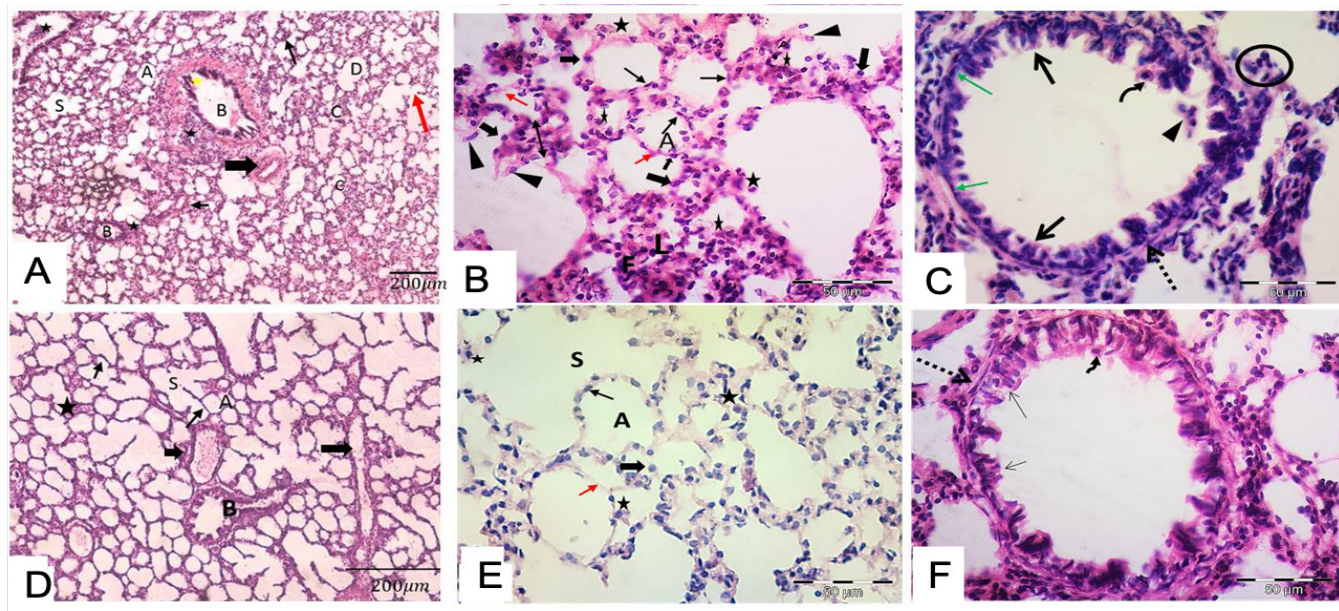


Fig.5: Representative photomicrographs of adult male albino rat lung tissue of the allicin oral (A-C) and allicin inhalation (D-F) groups showing: A) well-formed alveoli (A) and alveolar sacs (S) in some areas and other areas with collapsed (C) and dilated alveoli (D). Thick inter-alveolar septa (thin black arrow) in some areas and discontinuous interalveolar septum in other areas (red arrow). Notice the sloughed bronchial epithelium (B) (yellow star). Notice mild vascular congestion (thick arrow). B) Pneumocyte type I (thin arrows), numerous type II (thick arrows) and alveolar macrophages (black stars) separated with apparently normal interalveolar septum (red arrows). Notice thick interalveolar septum (double head arrow) with inflammatory cells mainly lymphocytes (L). Alveolar sacs begin to be divided internally by low ridges (arrowheads). Few fibroblasts (F) can be noticed in interstitial tissue. C) Partially restored bronchiolar epithelium (black arrows) with presence of flat cells among the epithelial cells (green arrows). Few desquamated epithelial cells (arrowhead) and macrophages (curved arrow) in the bronchiolar lumen. Notice partially restored circular smooth muscle layer (dotted arrow) with few inflammatory cell infiltration around the bronchiole (black circle). D) Apparently restored lung histological architecture. Most of alveoli (A) are patent separated by thin interalveolar septum (thin black arrows). Notice the bronchiole with apparently restored its epithelial lining (B). Few inflammatory cellular infiltration can be seen (black star). Vascular congestion and dilatation can be seen (thick arrow). E) Pneumocyte type I (thin black arrow), prominent type II (thick arrows) and alveolar macrophages (black star) separated by thin interalveolar septum (red arrows). F) Apparently normal bronchiolar epithelium with restored mucosal folding (thin arrows) and continuous circularly arranged smooth muscle layer (dotted arrow). Notice presence of macrophage in the bronchiolar lumen (curved arrow). H&E: A, D X100; B, C, E, F X400

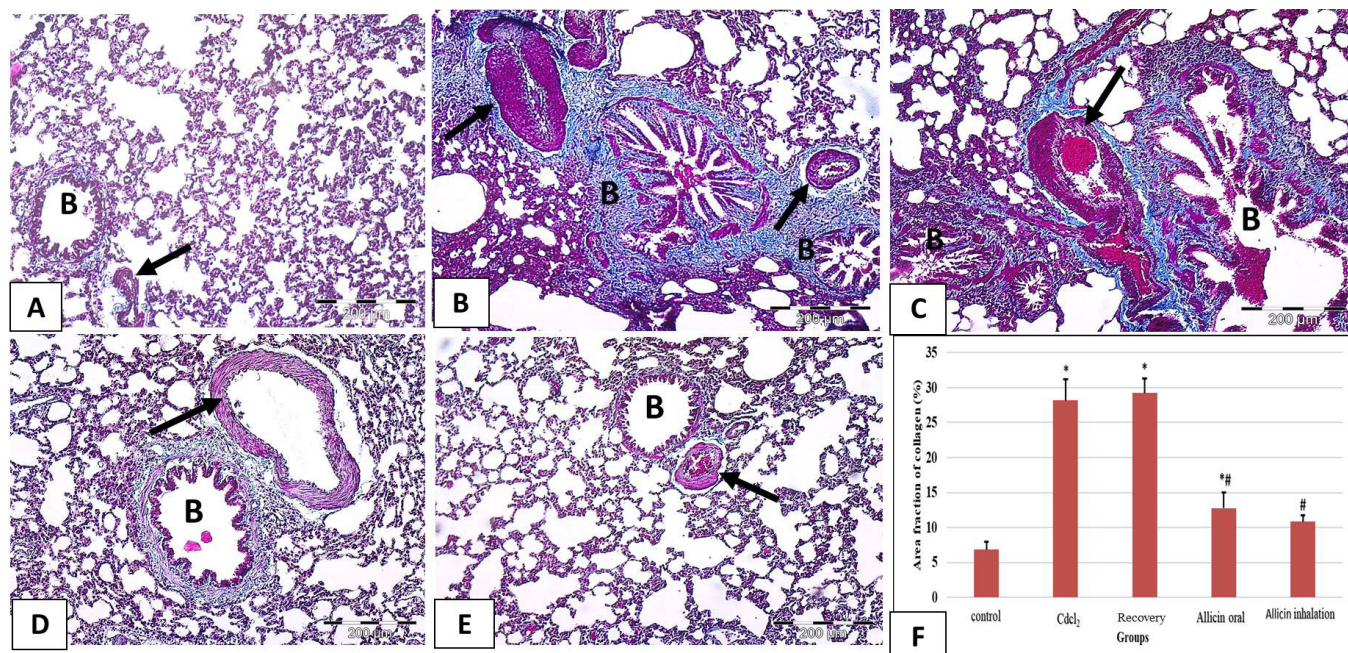


Fig. 6: Representative photomicrographs of adult male albino rat lung tissue of different groups showing collagen deposition in Cdcl₂ induced acute lung injury and the effect of allicin treatment: A) Control group showing minimal collagen deposition around the bronchiole (B) and the blood vessel (arrow). B) Cdcl₂ group and C) Recovery group showing marked increase in collagen deposition around the bronchioles (B) and the blood vessel (arrows). D) Allicin oral group showing mild collagen deposition around the bronchiole (B) and the blood vessel (arrow). E) Allicin inhalation group showing minimal collagen deposition around the bronchiole (B) and the blood vessel (arrow). F) The mean area fraction of collagen deposition in Masson trichrome stained sections in the studied groups (n = 8). * Significant vs: Control group, # Significant vs: Cdcl₂ group, & Significant vs: allicin oral group; significant at $p \leq 0.05$ Masson's trichrome X100

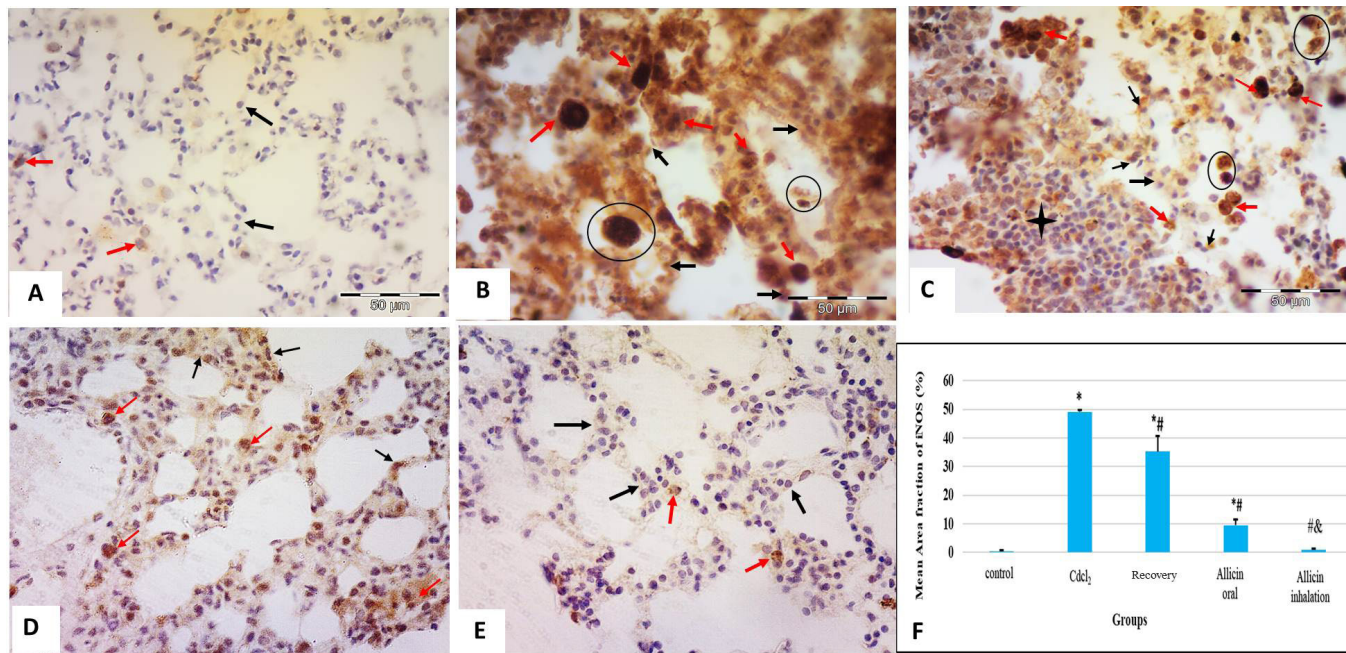


Fig. 7: Representative photomicrographs of adult male albino rat lung tissue immunohistochemically stained for iNOS showing: A) Control group with negative immune expression in the cells lining alveoli (black arrows) and faint expression in few cells in the inter-alveolar septa (red arrows). B) CdCl₂ group with strong positive immune expression in the cells lining the alveoli (black arrows), and in the cells in the inter-alveolar septa (red arrows). Notice immunopositive cells in the alveolar lumen (black circle). C) Recovery group with positive immune expression in the cells lining the alveoli (black arrows) and strong positive expression in the cells in the inter-alveolar septa (red arrows) as well as the interstitium (black star). Notice immunopositive cells in the alveolar lumen (black circle). D) Allicin oral group with faint expression in the cells lining the alveoli (black arrows) and positive immune expression in the cells in the inter-alveolar septa (red arrows). E) Allicin inhalation group with negative expression in the cells lining the alveoli (black arrows) and faint positive expression in scattered cells in the inter-alveolar septa (red arrows). F) The mean area fraction of iNOS immune reactivity of different groups (n = 8). * Significant vs: Control group, # Significant vs: CdCl₂ group, & Significant vs: allicin oral group; significant at $p \leq 0.05$. IHC by iNOS antibody X400

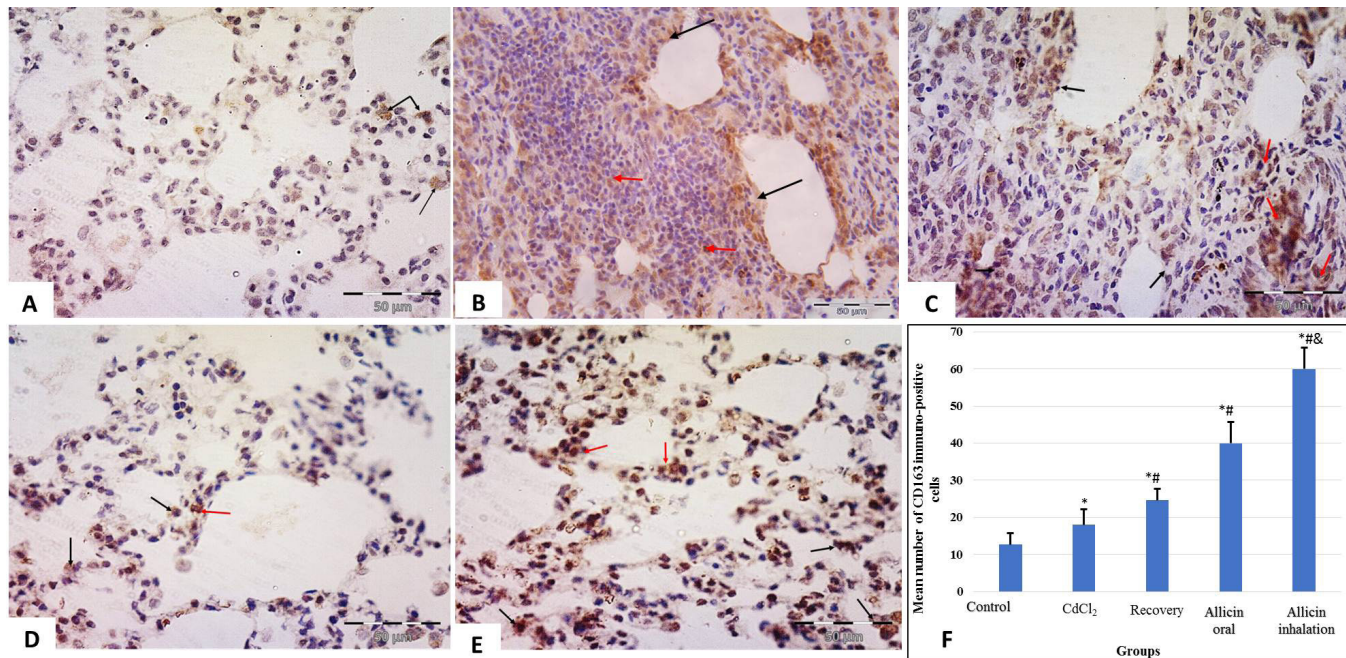


Fig. 8: Representative photomicrographs of adult male albino rat lung tissue immunohistochemically stained for CD163 antibodies showing: A) Control group with scanty CD163 positive macrophages in the alveolar wall (black arrows). B) CdCl₂ group with few CD163 positive macrophages in alveolar wall (black arrows) and in the interalveolar septum (red arrows). C) Recovery group with many CD163 positive macrophages in the alveolar wall (black arrows) and in the interstitium (red arrows). D) Allicin oral group with many CD163 positive macrophages in the alveolar wall (black arrows) and in the interalveolar septum (red arrow). E) Allicin inhalation group with numerous CD163 positive macrophages in the alveolar wall (black arrows) and in the interalveolar septum (red arrows). Notice large sized CD163 positive macrophages in the alveolar lumina (circle). F) The mean number of CD 163 immunopositive cells in different groups (n = 8). * Significant vs: Control group, # Significant vs: CdCl₂ group, & Significant vs: allicin oral group; significant at $p \leq 0.05$. IHC by CD163 antibody x400

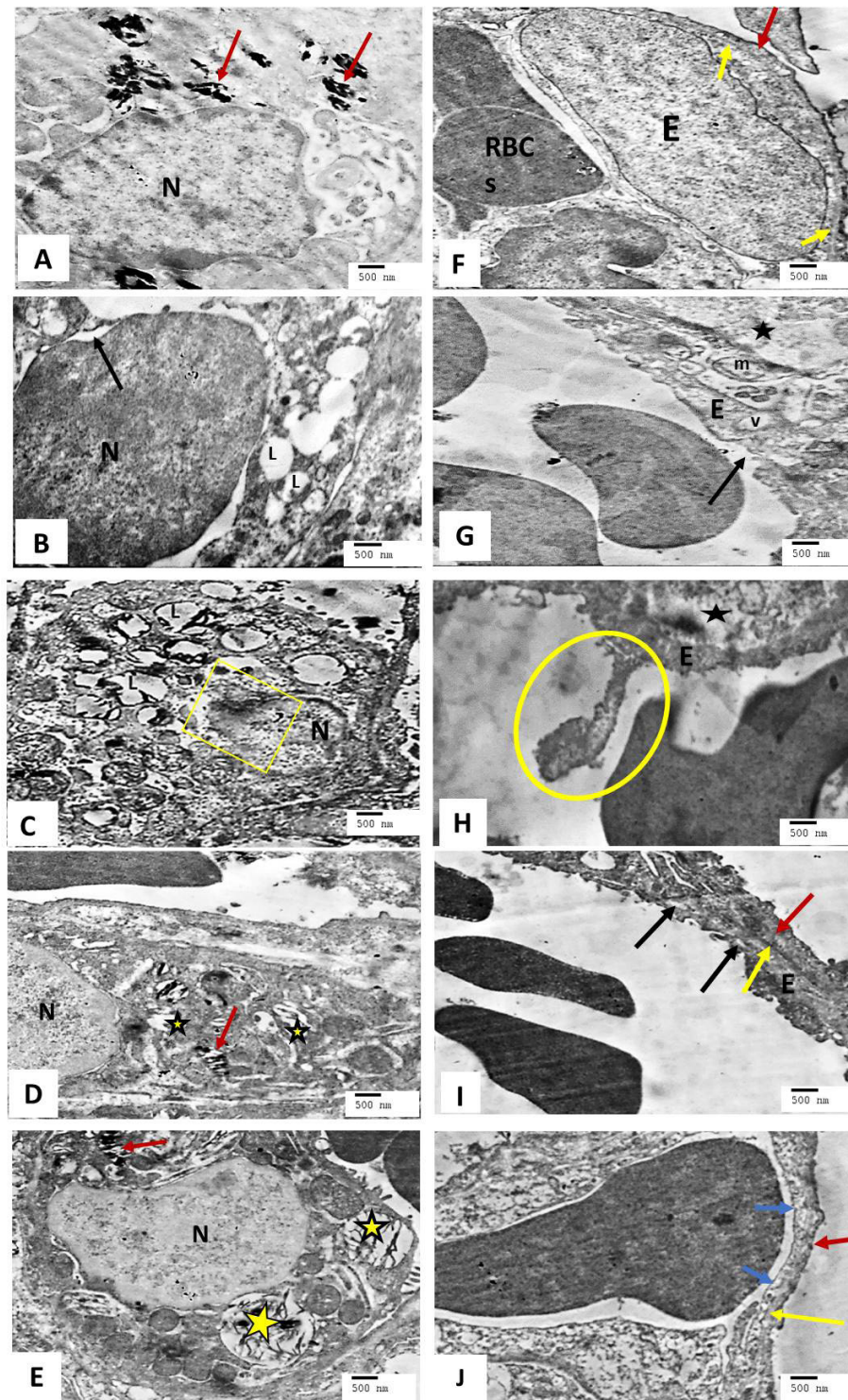


Fig 9: Representative electronmicrographs of an ultrathin section in the lung showing type II pneumocyte (A-E) and blood capillaries (F-J). A) Control group with numerous round to oval lamellar bodies (red arrows) and intact euchromatic nucleus (N). B) Cdcl2 group with heterochromatic nucleus (N), dilated perinuclear space (thin arrows) and empty lamellar bodies (L). C) Recovery group revealing degenerated lamellar bodies (L) with indistinct lamellation and shrunken heterochromatic nucleus (N) with disrupted nuclear membrane (boxed area). D) Allicin oral and E) allicin inhalation groups showing euchromatic nuclei (N), intact lamellar bodies (red arrows) and lamellar bodies with indistinct lamellation (stars). F) Control group showing blood capillary lined with endothelial cell (E) and containing red blood cells (RBCs). Notice type-I pneumocyte with thin attenuated cytoplasm (red arrow) and the fused basement membrane (FBM) (yellow arrows) between endothelial cell and type-I pneumocyte. G) Cdcl2 group revealing disruption (arrow), vacuolation (v) and swollen mitochondria with degenerated cristae (m) in the capillary endothelium (E) with degenerated type I pneumocyte (star). H) Recovery group showing sprout out (yellow circle) in cell membrane of endothelial cell (E) and degenerated type I pneumocyte (star). I) Allicin oral group revealing endothelial cell (E) with small cytoplasmic vacuoles (black arrows) and FBM (yellow arrow) between endothelial cell and type-I pneumocyte (red arrow). J) Allicin inhalation group with apparently normal capillary endothelium (blue arrows) with regular cytoplasm, apparently normal type I pneumocyte with thin attenuated cytoplasm (red arrow) and FBM (yellow arrow) between them. TEM: A, B, C, D, E, F, J X4000; G, H, I X5000

DISCUSSION

Great interest has been directed to acute lung diseases after the pandemic of corona virus as it harvests millions of people souls all over the world by the ghost of corona virus due to ARDS. Cadmium chloride inhalation is one of the established models of acute lung injury, it induces nearly the same histopathological findings as acute viral infection^[24]. There are accumulating data from the recent research work that allicin, the active ingredient of garlic, may be of great help as an adjuvant therapy in cases of ALI^[25].

In the present study, we induced ALI by CdCl₂ inhalation and investigate the possible therapeutic effects of allicin by 2 different routes (oral/ inhalation)^[19].

Our histological findings revealed that CdCl₂ inhalation induced marked distortion in the normal lung architecture with alveolar and bronchiolar epithelium damage and these results were reported also by^[26] who stated that CdCl₂ inhalation produced many detritus effects on lung tissue.

Marked inflammatory cells infiltrations were also observed within thickened interalveolar septum. Furthermore, the alveoli and bronchioles showed extravasated blood with areas of hemorrhage and congested dilated blood vessels^[27]. reported that CdCl₂ has a pro-inflammatory property^[28]. explained that the acute inflammation caused by CdCl₂ inhalation leads to increase in the vascular permeability, endothelial cells injury and inflammatory cells recruitment.

Similarly, coagulopathy is evident pathological feature of covid-19 infection which is associated with, endotheliopathy and vasculitis, the main cause of of ALI with alveolar epithelial damage^[29]

Homogenous acidophilic material was also observed inside some alveoli and within inter-alveolar septa and it has been explained by^[30] as plasma exudates produced of alveolar damage. The same findings were described in postmortem biopsies from patients with covid-19^[31]. In the present study, CdCl₂ tissue sections showed marked increase in collagen deposition. This was in accordance with^[32] who reported an important role of fibroblasts and macrophages in the replacement of the provisional matrix. On the other hand,^[33] hypothesized that apoptosis of the lung epithelial cells can induce pulmonary fibrosis through signaling pathway of caspase-3 activation.

Progressive fibrotic lung disease is one of the possible complications of covid-19 infection and it is one of the most serious long-term complications^[34].

Ultrastructure examination of CdCl₂ group tissue sections showed degenerative changes in pneumocyte II as heterochromatic nucleus, dilated perinuclear area, and empty lamellar bodies. These results agree with^[35] who reported similar findings in lung tissue with heavy metal exposure. These findings are also in agreement with^[36] who stated that cadmium administration was associated with DNA damage of lung cells.

CdCl₂ groups also showed disruption, vacuolation and sprout out in the endothelial lining of blood capillaries forming blood air barrier. This findings also found by^[37] in a human model of alveolarcapillary barrier with well differentiated and tight epithelial barrier exposed to Cd²⁺ resulted in disruption of protein E-cadherin of the tight junction between endothelial cells and finally led to breakdown of the epithelial barrier.

These ultrastructural changes were in accordance with^[38] who found similar degenerative changes in covid-19 autopsied patients.

As regard allicin treated groups, oral allicin administration showed improvement in the histological lung structure in the form of regeneration and restoration of alveolar and bronchial epithelium with decrease in vascular congestion and interstitial inflammatory cell infiltrations. Furthermore, significant decrease in collagen deposition was obviously observed. These beneficial effects were more evident with allicin inhalation which nearly showed normal lung architecture.

Ultrastructure examination of allicin treated groups revealed regeneration and restoration of normal structure of pneumocyte II as there were regenerated lamellar bodies, intact euchromatic nucleus and these findings were more evident in allicin inhalation group. These findings were in agreement with^[39].

Focusing on the endothelial lining of the blood air barrier in allicin treated groups showed apparently normal structure in allicin inhalation group. These findings were supported by^[40] who assessed the protective effect of allicin against ischemia and hypoxia that induced cardiomyocyte apoptosis.

To understand the underlying mechanisms of these deleterious effects of CdCl₂ and how can allicin improve these effects; we assessed tropomyosin receptor kinase B (TrkB), which is a receptor for brain-derived neurotrophic factor (BDNF)^[41] level in lung tissue. TrkB signaling is essential for alveolar organoid development, so TrkB receptor activation is important for the recovery from ALI^[42].

In addition, the BDNF is considered as a STAT3 target gene which is important for regeneration of type II pneumocyte cells. During lung repair, the type II alveolar pneumocytes act as a progenitor for new type II and type I alveolar pneumocytes^[42] which is aided by TrkB signaling activation^[43]. In our study, CdCl₂ group showed a significant decrease in TrkB level and this result was in agreement with^[44]. In lung tissue, TrkB is expressed in alveolar macrophages, type II pneumocytes and neuroepithelial bodies^[45]. These studies reported that CdCl₂ can induce apoptosis in type II pneumocytes through modulation of the cellular level of Ca²⁺, activation of caspases and nitrogen-activated protein kinases (MRPKs) in the cells and subsequently decrease TrkB level.

Alliin treated groups showed significant increase in TrkB levels in lung tissue especially in alliin inhalation group. This was in agreement with^[46] who stated that alliin administration helps in type II pneumocyte regeneration and decreased its apoptosis via culturing Human type II-like alveolar epithelial cells A549 in a media supplemented with LPS and alliin. They found that alliin administration significantly improved the A549 cell viabilities and reduced their apoptotic rate.

So, alliin is able to improve the viability of type II alveolar pneumocytes which is the main site of TrkB expression in lung tissue.

We also investigated the oxidative stress caused by CdCl₂ administration and anti-oxidant effect of alliin, levels of malonaldehyde (MDA), a biomarker of oxidative stress and lipid peroxidation^[47], (GSH) scavenger of reactive oxygen species and immunohistochemical iNOS antibody expression were assessed in different groups.

There was a significant elevation of malonaldehyde (MDA) level in CdCl₂ induced acute lung injury. This was in agreement with^[48] who explained that MDA is the main byproduct of lipid peroxidation which is a sensitive reaction to CdCl₂ toxicity, and it can be effectively linked to oxidative stress in tissues. Alliin inhalation was more superior on oral route and showed significant decrease in MDA levels and this was in agreement with^[49] who explained that alliin has the ability of quenching the free radicals, that may further decrease lipid peroxidation.

As regard GSH levels, CdCl₂ group showed significant decrease in its level when compare to the control group and this was in coincide with^[50] who explained that CdCl₂ toxicity is due to the depletion of antioxidant defense mechanisms which causes oxidative stress. Cadmium chloride may induce oxidative damage by increasing peroxidation of membrane lipid. Cd also binds preferentially to sulfhydryl group (-SH)-containing cellular molecules such as GSH^[51]. The depletion of -SH containing molecules that participate in detoxification and oxidative phosphorylation is an essential indirect mechanism of oxidative injury induced by Cd. These events eventually cause the accumulation of reactive oxygen species (ROS) (such as superoxide radicals, hydrogen peroxide and hydroxyl radicals) as well as lipid peroxides accumulation^[52].

And the same sequences of events have been reported in cases of covid 19^[53].

Interestingly, alliin groups showed marked increase in level of GSH when compared to CdCl₂ group especially in the inhalation group, this finding was in agreement with^[54]. Several studies suggested a direct antioxidant effect of alliin through interaction with hydroxylated molecules or transferring its allylic hydrogen to the oxidized peroxy radicals or indirect through stimulation of phase II detoxifying enzymes (hemeoxygenase-1, NAD(P) H-quinine oxidoreductase, glutathione-S-transferases and γ -glutamyl-cysteine synthetase) in a nuclear factor

related-2 (Nrf2)-dependent pathway^[55]. In addition, alliin has a potent role in the formation of 2-propenesulfenic acid which is a very potent antioxidant^[54].

iNOS shows constitutive expression in human airways by the inflammatory cells and activated macrophages and it is activated by a variety of proinflammatory cytokines including TNF- α , interferon γ , IL-6 and IL-1 on exposing lung parenchyma to oxidative-nitrative stress^[56]. iNOS was believed to play role in generating highly reactive ROS which cause various cellular damage. Our results showed significant increase in iNOS antibody expression in CdCl₂ groups compared with control group.

Found that the early response to CdCl₂ administration was persistent inflammation with presence of numerous proinflammatory macrophages that cause tissue damage through excessive release of NO^[57].

While alliin treated groups revealed significant decreased in iNOS antibody expression compared with in CdCl₂ groups especially in alliin inhalation group^[58] also suggested that alliin inhibits the production of inflammatory cytokines and subsequently inhibits iNOS release through both mRNA and protein level.

Immune cells including monocytes, macrophages and lymphocytes are the main sources of cytokine production. Some of these cytokines are pro-inflammatory facilitate inflammation while others are anti-inflammatory act as scavenger for the inflammatory process. One of the most important Inflammatory cytokines is interleukins (ILs) which are produced primarily for recruitment of leukocytes to the site of injury or infection^[59]. Cytokines regulate the immune response and modulate inflammation through a complex network of interactions. However, excessive inflammatory cytokine production can lead to serious complication as tissue damage, hemodynamic changes, multi-organ failure, and death^[60].

Interleukin 6 (IL-6) is an important pro-inflammatory cytokine that produced mainly from the pro-inflammatory macrophages^[61]. In this study, CdCl₂ group showed a significant increase in interleukin 6 level in lung tissue. Several studies reported that there was an increase in IL-6 levels in lung tissues^[62] as well as in the broncho-alveolar lavage^[63] of rats with ALI. It is documented that IL-6 react with heparin sulfate glycoprotein on the surface of vascular endothelial cell causing a potent chemotactic effect with subsequent adhesion between activate neutrophils and endothelial cells. Therefore, the release of IL-6 is considered to be an important factor in the pathogenesis of ALI^[64].

In this study, alliin treated groups showed significant decrease in IL-6 levels in lung tissue especially in alliin inhalation group and this was also evidenced by^[65] who reported the attenuating effect of alliin in lipopolysaccharide induced ALI in neonatal rats.

Alliin is reported to exhibit an immunomodulatory effect through stimulating certain cell types as anti-

inflammatory macrophages, NK cells and dendritic cells so that it can modulate cytokine secretion such as IL-6^[66]. Clinical data to date recommends to add IL-6 inhibitors (tocilizumab 8mg/kg intravenously 8mg/kg intravenously 8mg/kg intravenously) to the regimen of treatment in patients with covid-19^[67].

For more investigation of the immunomodulatory effect of allicin, we used CD163 anti-body to detect anti-inflammatory macrophages.

A significant increase in the mean number of CD163 positive cells in all the studied groups especially in allicin inhalation group was noticed. These results were explained by^[68] who reported that CD163+ macrophage population has been associated with anti-inflammatory functions of allicin and its expression is induced by the anti-inflammatory mediators IL-10 that released in response to allicin administration^[69], whereas the proinflammatory cytokines IL6, IFN- γ and TNF- α that released in response to CdCl₂ exposure suppress its expression^[57].

Other beneficial effects of allicin are its anticoagulant and anti-thrombotic effects. Allicin activates fibrinolytic action via acceleration of (tissue-type plasminogen activator) t-PA-mediated plasminogen activation, moreover it suppresses the coagulation system by inhibiting thrombin formation, suggesting an important role in preventing thrombus formation^[70].

From all previous results, we found that the inhalation route of allicin administration has superior effect than oral route and this explained by^[16] who stated that oral administration of allicin was difficult to provide its effective therapeutic concentrations so it is hard to achieve its function because it is titrated out by glutathione in the cells and blood.

While the direct inhalation of allicin vapor or aerosols potentially offered an immediate route for the treatment of lung pathogens in the case of lung infections as it can cross cell membranes easily and perform its function effectively^[25].

CONCLUSION

Based on the multifactorial mechanisms through which allicin inhalation improve the damaged lung tissues in ALI model, we recommend its use as an adjuvant therapy in treatment of ALI especially in COVID 19 pandemic.

FUNDING

This research did not receive any specific grant from funding agencies in the public, commercial, or not-for-profit sectors.

AVAILABILITY OF DATA AND MATERIALS

The data that support the findings of this study are available from the corresponding author upon reasonable request.

CONFLICT OF INTERESTS

There are no conflicts of interest.

REFERENCES

1. Abedi F, Hayes AW, Reiter R, Karimi GJPr. Acute lung injury: The therapeutic role of Rho kinase inhibitors. 2020;155:104736. DOI: 10.1016/j.phrs.2020.104736
2. Niethamer TK, Stabler CT, Leach JP, Zepp JA, Morley MP, Babu A, *et al.* Defining the role of pulmonary endothelial cell heterogeneity in the response to acute lung injury. 2020;9:e53072. DOI: 10.7554/eLife.53072
3. Du J, Li H, Lian J, Zhu X, Qiao L, Lin J. Stem cell therapy: a potential approach for treatment of influenza virus and coronavirus-induced acute lung injury. *Stem cell research & therapy.* 2020;11:1-9. DOI: 10.1186/s13287-020-01699-3
4. Deng B, Pakhomov O, Bozhok GJRMiB. Long-term effects of acute cadmium exposure on testis immune privilege. 2020;11(2):180-5. DOI: <https://doi.org/10.15421/022027>
5. Ali S, Bashir S, Mumtaz S, Shakir HA, Ara C, Ahmad F, *et al.* Evaluation of Cadmium Chloride-Induced Toxicity in Chicks Via Hematological, Biochemical Parameters, and Cadmium Level in Tissues. 2020:1-13. DOI: 10.1007/s12011-020-02453-9
6. Rafiei-Asl S, Khadjeh G, Jalali SM, Jamshidian J, Rezaie AJIVJ. Investigating the protective effects of bromelain against inflammatory marker alterations induced by cadmium pulmonary intoxication in rat. 2020;16(2):75-88. DOI: 10.22092/ari.2021.355559.1698
7. Wong AW, Fidler L, Marcoux V, Johannson KA, Assayag D, Fisher JH, *et al.* Practical considerations for the diagnosis and treatment of fibrotic interstitial lung disease during the coronavirus disease 2019 pandemic. *Chest.* 2020;158(3):1069-78. Doi: 10.1016/j.chest.2020.04.019
8. Albert RK, Smith B, Perlman CE, Schwartz DA. Is progression of pulmonary fibrosis due to ventilation-induced lung injury? *American journal of respiratory and critical care medicine.* 2019;200(2):140-51. Doi: 10.1164/rccm.201903-0497PP
9. Reiter J, Borlinghaus J, Dörner P, Schröder W, Gruhlke MC, Klaas M, *et al.* Investigation of the deposition behaviour and antibacterial effectivity of allicin aerosols and vapour using a lung model. 2020;19(2):1541-9. DOI: 10.3892/etm.2019.8387
10. Dai J, Chen Y, Jiang FJG. Allicin reduces inflammation by regulating ROS/NLRP3 and autophagy in the context of *A. fumigatus* infection in mice. 2020;762:145042. DOI: 10.1016/j.gene.2020.145042
11. Mösbauer K, Fritsch VN, Adrian L, Bernhardt J, Gruhlke MCH, Slusarenko AJ, *et al.* Allicin inhibits SARS-CoV-2 replication and abrogates the antiviral host response in the Calu-3 proteome. 2021. doi: <https://doi.org/10.1101/2021.05.15.444275>

12. Prajapati SK, Mishra G, Malaiya A, Jain A, Mody N, Raichur AM. Antimicrobial Application Potential of Phytoconstituents from Turmeric and Garlic. *Bioactive Natural Products for Pharmaceutical Applications*: Springer; 2021. p. 409-35. DOI: 10.1007/978-3-030-54027-2_12
 13. Vollmer AD. *Healing with DMSO: The Complete Guide to Safe and Natural Treatments for Managing Pain, Inflammation, and Other Chronic Ailments with Dimethyl Sulfoxide*: Ulysses Press; 2020.
 14. Asvadi S, Hayes JTA. Acute lung injury induced by cadmium aerosol. II. Free airway cell response during injury and repair. 1978;90(1):89. PMID: 619697
 15. Amer RM, Tahoon NMJ. The protective effect of folic acid and Vit B12 supplementation on albino rat lung injury due to cadmium inhalation. 2018;46(4):264. Doi: https://doi.org/10.4103/tmj.tmj_82_17
 16. Alam R, Fawzi EM, Alkhalf MI, Alansari WS, Aleya L, Abdel-Daim MM. Anti-inflammatory, immunomodulatory, and antioxidant activities of allicin, norfloxacin, or their combination against *Pasteurella multocida* infection in male New Zealand rabbits. *Oxidative medicine and cellular longevity*. 2018;2018. DOI: 10.1155/2018/1780956
 17. Aziz MY, Hussain SH, Ishak AR, Abdullah MA, Mohamed R, Ruzi II, *et al.* Heavy Metal Concentrations in Malaysian Adults' Hair and Associated Variables in Bukit Mertajam, Penang, Malaysia. 2021:1-7. DOI: 10.1007/s12011-021-02942-5
 18. Zhao S, Yang Q, Yu Z, Lv Y, Zhi J, Gustin P, *et al.* Protective effects of tiotropium alone or combined with budesonide against cadmium inhalation induced acute neutrophilic pulmonary inflammation in rats. *Plos one*. 2018;13(2):e0193610. DOI: 10.1371/journal.pone.0193610
 19. Xu W, Li X-p, Li E-z, Liu Y-f, Zhao J, Wei L-n, *et al.* Protective Effects of Allicin on ISO-Induced Rat Model of Myocardial Infarction via JNK Signaling Pathway. 2020;105(9-10):505-13. DOI: 10.1159/000503755
 20. Paris AJ, Hayer KE, Oved JH, Avgousti DC, Toulmin SA, Zepp JA, *et al.* STAT3–BDNF–TrkB signalling promotes alveolar epithelial regeneration after lung injury. 2020;22(10):1197-210. DOI: 10.1038/s41556-020-0569-x
 21. Deng G, He H, Chen Z, OuYang L, Xiao X, Ge J, *et al.* Lianqinjiedu decoction attenuates LPS-induced inflammation and acute lung injury in rats via TLR4/NF- κ B pathway. 2017;96:148-52. Doi: 10.1016/j.biopha.2017.09.094
 22. Suvarna KS, Layton C, Bancroft JD. *Bancroft's theory and practice of histological techniques* E-Book: Elsevier health sciences; 2018. eBook ISBN: 9780702068867
 23. Suvik A, Effendy AJMJVR. The use of modified Masson's trichrome staining in collagen evaluation in wound healing study. 2012;3(1):39-47.
 24. Rani A, Kumar A, Lal A, Pant MJ. Cellular mechanisms of cadmium-induced toxicity: a review. 2014;24(4):378-99. DOI: 10.1080/09603123.2013.835032
 25. Reiter J, Levina N, Van der Linden M, Gruhlke M, Martin C, Slusarenko AJ. Diallylthiosulfinate (Allicin), a volatile antimicrobial from garlic (*Allium sativum*), kills human lung pathogenic bacteria, including MDR strains, as a vapor. *Molecules*. 2017;22(10):1711. DOI: 10.3390/molecules22101711
 26. Zhao S, Yang Q, Yu Z, Lv Y, Zhi J, Gustin P, *et al.* Protective effects of tiotropium alone or combined with budesonide against cadmium inhalation induced acute neutrophilic pulmonary inflammation in rats. 2018;13(2):e0193610. DOI: 10.1371/journal.pone.0193610
 27. Mumtaz F, Albeltagy RS, Diab MS, Moneim AEA, Ola H. Exposure to arsenite and cadmium induces organotoxicity and miRNAs deregulation in male rats. *Environmental Science and Pollution Research*. 2020:1-10. DOI: 10.1007/s11356-020-08306-1
 28. Das SC, Al-Naemi HA. Cadmium toxicity: oxidative stress, inflammation and tissue injury. 2019. Doi: <https://doi.org/10.4236/odem.2019.74012>
 29. Iba T, Connors JM, Levy JH. The coagulopathy, endotheliopathy, and vasculitis of COVID-19. 2020:1-9. Doi: 10.1007/s00011-020-01401-6
 30. Hafez MS. Effect of selenium supplementation on the structure of the lung of adult albino rats subjected to experimentally induced chronic renal failure. *Egyptian Journal of Histology*. 2012;35(3):573-86. DOI: 10.1097/01.EHX.0000418500.63751.b7
 31. Xu Z, Shi L, Wang Y, Zhang J, Huang L, Zhang C, *et al.* Pathological findings of COVID-19 associated with acute respiratory distress syndrome. 2020;8(4):420-2. DOI: 10.1016/S2213-2600(20)30076-X
 32. Chambers RC, Mercer PF. Mechanisms of alveolar epithelial injury, repair, and fibrosis. 2015;12(Supplement 1):S16-S20. Doi: 10.1513/AnnalsATS.201410-448MG
 33. Predescu SA, Zhang J, Bardita C, Patel M, Godbole V, Predescu DN. Mouse lung fibroblast resistance to Fas-mediated apoptosis is dependent on the baculoviral inhibitor of apoptosis protein 4 and the cellular FLICE-inhibitory protein. 2017;8:128. DOI: 10.3389/fphys.2017.00128
 34. Ali RMM, Ghonimy MBIJEJoR, Medicine N. Post-COVID-19 pneumonia lung fibrosis: a worrisome sequelae in surviving patients. 2021;52(1):1-8. doi: 10.1186/s43055-021-00484-3
-

35. Bai YN, Ma L, Wang QY, Pu HQ, Zhang XP, Wu XJ, *et al.* The mechanism of acute lung injury induced by nickel carbonyl in rats. 2013;7(26):625-8. DOI: 10.3967/0895-3988.2013.07.018
36. Bishop E, Breheny D, Dillon D, Meredith CJTL. Toxicity of cadmium chloride in a 28-day repeated exposure human bronchial epithelial cell model. 2013(221):S163. DOI: 10.1016/j.toxlet.2013.05.349
37. Papritz M, Pohl C, Wübbecke C, Moisch M, Hofmann H, Hermanns MI, *et al.* Side-specific effects by cadmium exposure: apical and basolateral treatment in a coculture model of the blood–air barrier. 2010;245(3):361-9. DOI: 10.1016/j.taap.2010.04.002
38. Santana MF, Ferreira LCdLJRBdEM. From autopsy rooms and microscopes to life: informal mentoring in a pathology medical residency program. 2021;45. DOI: <https://doi.org/10.1590/1981-5271v45.supl.1-20210118>
39. Sánchez-Gloria JL, Martínez-Olivares CE, Rojas-Morales P, Hernández-Pando R, Carbo R, Rubio-Gayosso I, *et al.* Anti-Inflammatory Effect of Allicin Associated with Fibrosis in Pulmonary Arterial Hypertension. 2021;22(16):8600. DOI: 10.3390/ijms22168600
40. Ma L, Chen S, Li S, Deng L, Li Y, Li HJE-BC, *et al.* Effect of allicin against ischemia/hypoxia-induced H9c2 myoblast apoptosis via eNOS/NO pathway-mediated antioxidant activity. 2018;2018. Doi: 10.1155/2018/3207973
41. Ortiz-López L, González-Olvera JJ, Vega-Rivera NM, García-Anaya M, Carapia-Hernández AK, Velázquez-Escobar JC, *et al.* Human neural stem/progenitor cells derived from the olfactory epithelium express the TrkB receptor and migrate in response to BDNF. *Neuroscience*. 2017;355:84-100. DOI: 10.1016/j.neuroscience.2017.04.047
42. Nabhan AN, Brownfield DG, Harbury PB, Krasnow MA, Desai TJ. Single-cell Wnt signaling niches maintain stemness of alveolar type 2 cells. *Science*. 2018;359(6380):1118-23. DOI: 10.1126/science.aam6603
43. Paris AJ, Hayer KE, Oved JH, Avgousti DC, Toulmin SA, Zepp JA, *et al.* STAT3–BDNF–TrkB signalling promotes alveolar epithelial regeneration after lung injury. *Nature cell biology*. 2020;22(10):1197-210. DOI: 10.1038/s41556-020-0569-x
44. Ben Mimouna S, Le Charpentier T, Lebon S, Van Steenwinckel J, Messaoudi I, Gressens P. Involvement of the synapse-specific zinc transporter ZnT3 in cadmium-induced hippocampal neurotoxicity. *Journal of cellular physiology*. 2019;234(9):15872-84. DOI: 10.1002/jcp.28245
45. García-Suárez O, Pérez-Pinera P, Laurà R, Germanà A, Esteban I, Cabo R, *et al.* TrkB is necessary for the normal development of the lung. *Respiratory physiology & neurobiology*. 2009;167(3):281-91. DOI: 10.1016/j.resp.2009.06.001
46. Zheng Y, Cai W, Yan G, Xu Y, Zhang M-q. Allicin protects against lipopolysaccharide-induced acute lung injury by up-regulation of claudin-4. *Tropical Journal of Pharmaceutical Research*. 2014;13(7):1063-9. Doi: 10.4314/tjpr.v13i7.8
47. Lei J, Wei Y, Song P, Li Y, Zhang T, Feng Q, *et al.* Cordycepin inhibits LPS-induced acute lung injury by inhibiting inflammation and oxidative stress. *European Journal of Pharmacology*. 2018;818:110-4. DOI: 10.1016/j.ejphar.2017.10.029
48. Sharma S, Kumari A. Protective effect of Curcuma longa administration on lung of mice exposed to cadmium. *Asian Journal of Pharmaceutical and Clinical Research*. 2018;536-9. DOI: <https://doi.org/10.22159/ajpcr.2018.v11i10.29010>
49. Sun D, Sun C, Qiu G, Yao L, Yu J, Al Sberi H, *et al.* Allicin mitigates hepatic injury following cyclophosphamide administration via activation of Nrf2/ARE pathways and through inhibition of inflammatory and apoptotic machinery. *Environmental Science and Pollution Research*. 2021;1-12. DOI: 10.1007/s11356-021-13392-w
50. Elkhadragy MF, Kassab RB, Metwally D, Almeer RS, Abdel-Gaber R, Al-Olayan EM, *et al.* Protective effects of *Fragaria ananassa* methanolic extract in a rat model of cadmium chloride-induced neurotoxicity. *Bioscience reports*. 2018;38(6). Doi: 10.1042/BSR20180861
51. Abdeen A, Abou-Zaid OA, Abdel-Maksoud HA, Aboubakr M, Abdelkader A, Abdelnaby A, *et al.* Cadmium overload modulates piroxicam-regulated oxidative damage and apoptotic pathways. *Environmental Science and Pollution Research*. 2019;26(24):25167-77. DOI: 10.1007/s11356-019-05783-x
52. Wang J, Zhu H, Wang K, Yang Z, Liu Z. Protective effect of quercetin on rat testes against cadmium toxicity by alleviating oxidative stress and autophagy. *Environmental Science and Pollution Research*. 2020;27(20):25278-86. DOI: 10.1007/s11356-020-08947-2
53. Chernyak BV, Popova EN, Zinovkina LA, Lyamzaev KG, Zinovkin RAJFiP. Mitochondria as Targets for Endothelial Protection in COVID-19. 2020;11. Doi: 10.3389/fphys.2020.606170
54. Borlinghaus J, Kappler U, Antelmann H, Noll U, Gruhlke MC, Slusarenko AJ. Allicin, the odor of freshly crushed garlic: A review of recent progress in understanding allicin's effects on cells. *Molecules*. 2021;26(6):1505. DOI: 10.3390/molecules26061505

55. Abdel-Daim MM, Khalifa HA, Ahmed AA. Allicin ameliorates doxorubicin-induced cardiotoxicity in rats via suppression of oxidative stress, inflammation and apoptosis. *Cancer chemotherapy and pharmacology*. 2017;80(4):745-53. DOI: 10.1007/s00280-017-3413-7
56. Liu W-w, Han C-h, Zhang P-x, Zheng J, Liu K, Sun X-j. Nitric oxide and hyperoxic acute lung injury. *Medical gas research*. 2016;6(2):85. Doi: 10.4103/2045-9912.184718
57. Kassab RB, Lokman MS, Daabo HM, Gaber DA, Habotta OA, Hafez MM, *et al.* Ferulic acid influences Nrf2 activation to restore testicular tissue from cadmium-induced oxidative challenge, inflammation, and apoptosis in rats. *Journal of Food Biochemistry*. 2020;44(12):e13505. DOI: 10.1111/jfbc.13505
58. Qian Y-Q, Feng Z-H, Li X-B, Hu Z-C, Xuan J-W, Wang X-y, *et al.* Downregulating PI3K/Akt/NF- κ B signaling with allicin for ameliorating the progression of osteoarthritis: *in vitro* and *vivo* studies. *Food & function*. 2018;9(9):4865-75. DOI: 10.1016/j.intimp.2019.105953
59. Turner MD, Nedjai B, Hurst T, Pennington DJ. Cytokines and chemokines: At the crossroads of cell signalling and inflammatory disease. *Biochimica et Biophysica Acta (BBA)-Molecular Cell Research*. 2014;1843(11):2563-82. Doi: <https://doi.org/10.1016/j.bbamcr.2014.05.014>
60. Liu Z, Wang Y, Wang Y, Ning Q, Zhang Y, Gong C, *et al.* Dexmedetomidine attenuates inflammatory reaction in the lung tissues of septic mice by activating cholinergic anti-inflammatory pathway. *International immunopharmacology*. 2016;35:210-6. DOI: 10.1016/j.intimp.2016.04.003
61. Chen L, Deng H, Cui H, Fang J, Zuo Z, Deng J, *et al.* Inflammatory responses and inflammation-associated diseases in organs. *Oncotarget*. 2018;9(6):7204. doi: 10.18632/oncotarget.23208
62. Hu X, Kim K-h, Lee Y, Fernandes J, Smith MR, Jung Y-J, *et al.* Environmental cadmium enhances lung injury by respiratory syncytial virus infection. *The American journal of pathology*. 2019;189(8):1513-25. DOI: 10.1016/j.ajpath.2019.04.013
63. Liu X, Yang J, Li J, Xu C, Jiang W. Vanillin Attenuates Cadmium-Induced Lung Injury Through Inhibition of Inflammation and Lung Barrier Dysfunction Through Activating AhR. *Inflammation*. 2021:1-10. DOI: 10.1007/s10753-021-01492-1
64. Re SL, Dumoutier L, Couillin I, Van Vyve C, Yakoub Y, Uwambayinema F, *et al.* IL-17A-producing $\gamma\delta$ T and Th17 lymphocytes mediate lung inflammation but not fibrosis in experimental silicosis. *The Journal of Immunology*. 2010;184(11):6367-77. DOI: 10.4049/jimmunol.0900459
65. Wang X, Zhang C, Chen C, Guo Y, Meng X, Kan C. Allicin attenuates lipopolysaccharide-induced acute lung injury in neonatal rats via the PI3K/Akt pathway. *Molecular medicine reports*. 2018;17(5):6777-83. DOI: 10.3892/mmr.2018.8693
66. Arreola R, Quintero-Fabián S, López-Roa RI, Flores-Gutiérrez EO, Reyes-Grajeda JP, Carrera-Quintanar L, *et al.* Immunomodulation and anti-inflammatory effects of garlic compounds. 2015;2015. Doi: 10.1155/2015/401630
67. Alzghari SK, Acuña VSJJoCV. Supportive treatment with tocilizumab for COVID-19: a systematic review. 2020;127:104380. DOI: 10.1016/j.jcv.2020.104380
68. Enomoto Y, Suzuki Y, Hozumi H, Mori K, Kono M, Karayama M, *et al.* Clinical significance of soluble CD163 in polymyositis-related or dermatomyositis-related interstitial lung disease. *Arthritis research & therapy*. 2017;19(1):1-9. DOI: 10.1186/s13075-016-1214-8
69. Deng X, Yang P, Gao T, Liu M, Li X. Allicin attenuates myocardial apoptosis, inflammation and mitochondrial injury during hypoxia-reoxygenation: an *in vitro* study. *BMC Cardiovascular Disorders*. 2021;21(1):1-9. DOI: 10.1186/s12872-021-01918-6
70. Hussein HJ, Hameed IH, Hadi MY. A Review: Anti-microbial, Anti-inflammatory effect and Cardiovascular effects of Garlic: *Allium sativum*. *Research Journal of Pharmacy and Technology*. 2017;10(11):4069-78. DOI: 10.5958/0974-360X.2017.00738.7
-

الملخص العربي

التأثير التحسيني المحتمل للأليسين (عن طريق الفم/استنشاق) على الإصابة الرئوية الحادة المحدثة بالكاديوم في ذكور الجرذان البيضاء البالغة: دراسة هستولوجية وهستو-كيميائية مناعية

اميرة فتحي احمد ، ريهام محمد أبو الليل ، سحر احمد مخيمر، سها عبد القوي عبد الوهاب

قسم الهستولوجي وبيولوجيا الخلية، كلية الطب، جامعة المنيا، المنيا

مقدمة: يعد ايجاد العلاج المناسب لإصابة الرئة الحادة أحد أهم التحديات الصحية في الوقت الحاضر خاصة انها تمثل أخطر مضاعفات فيروس كورونا (COVID-19) والسبب الرئيسي للوفاة. تعددت الدراسات حول الآثار العلاجية المحتملة لمركب الأليسين (المادة الفعالة في الثوم) في علاج الكثير من حالات أمراض الجهاز التنفسي. **الهدف:** أظهرت الدراسة الحالية وللمرة الأولى طريقة جديدة لتناول الأليسين والتي تحسن بشكل ملحوظ آثاره العلاجية في النموذج الحيواني المستحث لإصابة الرئة الحادة.

الطرق ومواد البحث: تم تقسيم أربعين من ذكور الجرذان البيضاء إلى المجموعات التالية: مجموعة ضابطة، ومجموعة النموذج الحيواني لإصابة الرئة الحادة المستحث باستنشاق كلوريد الكاديوم، ومجموعة لإصابة الرئة الحادة تركت دون علاج ومجموعتين معالجتين بتناول الأليسين بطريقتين مختلفتين، احدهما عن طريق الفم والاخرى خلال استنشاق البخاخات بجرعة ٢٠٠ مجم / كجم.

النتائج: تسبب استنشاق كلوريد الكاديوم في حدوث التهابات واحتقان في الأوعية الدموية وكثير من التغييرات النسيجية المرضية المشابهة للتغيرات الحادثة في خزعة الرئة المصابة بفيروس كورونا (COVID-19). وأدى الأليسين إلى تحسين هذه التأثيرات الضارة بشكل ملحوظ من خلال استنشاق البخاخات حيث تسبب في انخفاض ذي دلالة احصائية في الانترليوكين-٦ والانزيم المخلق للنيتريك اوكسيد والمالونداهيد مع زيادة ذات دلالة احصائية في عدد البلاعم الإيجابية لمضادات الالتهابات مجموعة التمايز ١٦٣. علاوة على ذلك، فقد تم تحفيز تجدد الخلايا الرئوية من النوع الثاني وهذا ما تم اكتشافه بواسطة علامة انتشار TrkB. كما أظهر مستوى الجلوتاثيون المضاد للأكسدة زيادة ذات دلالة احصائية مع استنشاق الأليسين. تحسنت البنية النسيجية للرئة بشكل ملحوظ وعادت تقريباً إلى وضعها الطبيعي بعد استنشاق الأليسين.

الخلاصة: خلصنا إلى أن الأليسين من خلال استنشاق البخاخات قد يكون مفيداً بشكل كبير في إدارة الحالات الحرجة مع إصابة الرئة الحادة.